

**Palaeobiological and geochemical aspects of reptilian coprolites from a Maastrichtian Deccan volcano-sedimentary intertrappean deposit of central India**

Vivesh V. Kapur<sup>a,b\*</sup>, Ramanand Sagar<sup>a,b</sup>, Kamlesh Kumar<sup>a,b</sup>, Amritpal Singh Chaddha<sup>a</sup>,  
Ranjit Singh Lourembam<sup>c</sup>, Anshika Mishra<sup>a, d</sup>, Anupam Sharma<sup>a</sup>

<sup>a</sup> Birbal Sahni Institute of Palaeosciences, 53, University Road, Lucknow 226007, India.

<sup>b</sup> Academy of Scientific and Innovative Research (AcSIR), Ghaziabad 201002, India.

<sup>c</sup> Centre for Advanced Studies in Geology, Panjab University, Chandigarh 160014, India.

<sup>d</sup> B-471, Rajajipuram, Lucknow 226017, India.

\* Corresponding author: Vivesh V. Kapur (Orcid ID: 0000-0001-6542-5964)

Email: [viveshkapur@gmail.com](mailto:viveshkapur@gmail.com); [viveshvir\\_kapur@bsip.res.in](mailto:viveshvir_kapur@bsip.res.in)

## ABSTRACT

Cretaceous-Paleogene coprolite (fossilized faecal matter) records are significant in terms of providing direct palaeobiological evidence (as inclusions) in order to understand the diet and linkage(s) to producer animal(s). In the past >150 years, research investigations (in India) have focussed on the Maastrichtian Type-A coprolite morphotype (linked to titanosaurid dinosaurs). Consequently, scanty information is available on the overall assemblage of Indian Maastrichtian vertebrate coprolites in terms of their morphological diversity, chemical composition, biotic-abiotic inclusions in the context of producer linkage(s) and geographic distribution within the Deccan volcano-sedimentary infra- and intertrappean deposits of India. Therefore, we here present a detailed record of a coprolite assemblage from the Maastrichtian intertrappean deposits of Lotkheri, central India. The investigated coprolite assemblage consists of five morphotypes based on their geometry, surface, and internal textures. Biotic inclusions suggest that chelonians and crocodiles are the most likely producers of these ichnofossils. The associated faunal remains of chelonians and crocodilians support the proposed producer linkages. Bite marks of Gar fish (genus *Lepisosteus*) observed on the external surface of a few coprolite specimens (studied herein) are rare in the global fossil records. The analytical evidences confirm the phosphatic composition of the coprolites with the unique presence of three distinct morphologies (i.e., spherical, rods, and needles) of hydroxyapatite crystal inclusions that are explained with the help of a chemical ‘Growth Unit Model’.

**Keywords:** Chelonians, Crocodiles, Hydroxyapatite, Ichnofossils, Palaeodiet

## INTRODUCTION

Coprolites (fossilised faecal matter) have been significantly utilized in several research studies to reconstruct past ecosystems and to understand the dietary habit(s) of prehistoric fauna (Richter & Baszio 2001a, 2001b; Chin 2002; Prasad et al. 2005; Zatoń et al. 2015; Khosla et al. 2015; Vajda et al. 2016; Chin et al. 2017; Qvarnström et al. 2017; Dentzien-Dias et al. 2018; Barrios-de Pedro et al. 2018; Bajdek & Bienkowska-Wasiluk 2020; Rummy et al. 2021; Yao et al. 2022). In this regard, vertebrate coprolites from the Cretaceous-Paleogene (K-Pg) interval are known to be significant in order to understand the change(s) in palaeodietary preference(s) of producer taxa and their surrounding palaeoecological condition(s) (Suazo et al. 2012) considering the prevalence of stressed climatic and/or environmental conditions near the K-Pg time-slice. It is generally argued that the climatic change(s) close to the K-Pg interval occurred as a result of a meteorite impact (at Chicxulub, Mexico) and/or extensive volcanic activity (e.g., Deccan Trap volcanism in India) (see Keller et al. 2020 and references therein). The Deccan volcanic activity occurred in three episodes/phases and straddled the K-Pg boundary spanning at least >5 million years (from 69 Ma to 63 Ma) (Pande 2002; Self et al. 2008; Schoene et al. 2015; Fantasia et al. 2016; Keller et al. 2020). The Maastrichtian Deccan Volcano Sedimentary Sequences (DVSS) i.e., the infratrappean (Lameta Formation) and the intertrappean deposits have yielded abundant data on various fossil vertebrate groups that include fish, reptiles, amphibians, and mammals (Kapur and Khosla 2019 and references therein). However, we have limited knowledge on Maastrichtian vertebrate coprolites in terms of their morphological diversity, chemical composition, biotic-abiotic inclusion(s), producer linkage(s), and geographic distribution within the DVSS in India. This is owing to but not limited to the following factors: a) sporadic and limited occurrence of DVSS, b) plausible preservation bias between coprolite ichnofossils and vertebrate body fossils, and c) scarce palaeontological efforts for the

recovery of coprolite ichnofossils within DVSS. Thus, much emphasized are the Maastrichtian Type-A coprolite morphotype (linked to titanosaurid dinosaurs) limited to an infratrappean (Lameta Formation) horizon at Pisdura locale, central India (Matley 1939; Prasad et al. 2005; Khosla et al. 2015; also refer to Table 1 in Kapur et al. 2020). Additionally, Maastrichtian ‘intertrappean’ coprolite data, to date, is represented by a single morphotype and limited to the Lotkheri locale, central India (refer to Kapur et al. 2006). Further, previously recorded reptilian coprolites (in particular, the ones linked to chelonians and crocodiles) from the infratrappean Pisdura locale (Matley, 1939) and the intertrappean deposits of Lotkheri (Kapur et al., 2006) have not been analysed, for their biotic/abiotic inclusions, and geochemical composition. The above-mentioned aspects do hamper our understanding on the morphometric/morphotaxonomic diversity of coprolite records from the Maastrichtian of India, the dietary habit(s) of the producer animal(s), and in a few cases envisaged association(s) of previously reported coprolites to producer taxa. We herein present a detailed account on coprolite assemblage recovered from a Maastrichtian intertrappean deposit at Lotkheri, central India. Data on biotic inclusion(s) assisted to infer the likely producer(s) and the producer(s) dietary habit(s). Analytical techniques helped to decipher the chemical composition of the recovered coprolites, host (coprolite-yielding), and associated lithologies. Finally, an attempt has been made to explain the unique presence of a variety of morphologies of hydroxyapatite crystal (observed as coprolite inclusions) in the context of a chemical model.

## **GEOLOGICAL SETTING AND AGE**

All the coprolites recorded in the present study were recovered as surface collections from an intertrappean site (geographic co-ordinates: N 24°29'; E 75°43') located ~0.5 km south of the village Lotkheri (also known as ‘Lotkhedi’), Bhanpura Tehsil, Mandsaur District, Madhya Pradesh State, central India (Figs. 1a-e). The sedimentary succession exposed at the Lotkheri

locality comprises a 0.75 m to 1.5 m variably thick unfossiliferous red clays overlain by a 0.30 m to 0.65 m ossiferous (coprolite- and vertebrate-yielding) grey-green clays (Figs. 1b-d). Underlying weathered basalts can be observed both in a nala section as well in a dug well within the vicinity of the Lotkheri fossil locale that hint at the ‘intertrappean’ nature of the studied sedimentary succession (Figs. 1e). Published literature suggest an absence of infratrappean (Lameta Formation) sediments in the vicinity of the investigated locality while the Deccan Traps are underlain by Vindhyan or the Lower Gondwana (Antroli Formation, equivalent to Talchir Boulder Beds) sediments (Kapur et al. 2006 and references therein). Based on the widely occurring intertrappean faunal remains (i.e., the presence of fish dental remains assigned to *Igdabatis indicus*, fish scales belonging to *Lepisosteus indicus*, chelonians and crocodilian remains) the Deccan volcano-sedimentary intertrappean deposits at Lotkheri are considered to be Maastrichtian in age (Kapur et al. 2006).

## **MATERIAL AND METHODS**

Surface prospecting at Lotkheri intertrappean site yielded a total of fourteen coprolite specimens, a rarity in terms of the coprolite data from the Maastrichtian ‘intertrappean’ horizons of India. The collected coprolite specimens were individually photographed with the help of a digital camera (Model: Nikon D5200) and measured using a Dial Vernier Calliper. The specimens were individually examined for external structures under a binocular microscope (Model: Leica S8APO) in the Vertebrate Palaeontology and Preparation Laboratory (VPPL), Birbal Sahni Institute of Palaeosciences (BSIP), Lucknow, India. Before the thin section, Scanning Electron Microscopy (SEM) and chemical analyses, the individual coprolite specimens were disinfected in a Sodium Perborate Monohydrate solution. To examine coprolite inclusions under an automated slide scanner (Model: Grundium Ocus MGU-00001) at VPPL, thin sections (30 µm thick and transverse to the long axis) of the coprolite specimens were prepared. Separately, a few coprolite specimens were chemically

examined utilizing Energy Dispersive Spectroscopy (EDS) (at multiple spots) and a Scanning Electron Microscope (Model: JEOL7610F) under the acceleration voltage of 15kv and variable (6-9 A) current with EDAX (Model: Octane Plus with TEAM software version V4.2.1) at BSIP, Lucknow, India. Prior to XRD analysis, the coprolite specimens were cleaned utilizing an ultrasonic cleaner. Individual coprolite specimens, associated- (LTK-1) and host-lithology (LTK-2) samples were grounded up to 74 $\mu$ m. All the grounded specimens/samples were analysed using Panalytical X'pert<sup>3</sup> powder diffractometer equipment, working at 45 KV & 40 mA. The XRD measurements were carried out from 5° to 70° (2 $\theta$ ) range with a step size of 0.010° and time per step 30s with a scan speed of 0.090°/s using Cu as X-ray source ( $K\alpha=1.5405\text{\AA}$ ) at the BSIP, Lucknow, India. The mineral identification was carried out by the X'pert high score (<https://www.malvernpanalytical.com>) and ICDD PDF-4 mineral database (Gates-Rector and Blanton 2019). In addition, the two sediment samples (i.e., LTK-1 & LTK-2) were analysed by the X-ray Fluorescence (XRF) technique (WD-XRF Model: Axios max, 4 KW, PANalytical) at BSIP, Lucknow, India. The precision and accuracy of the sample preparation and instrumental performance were checked using international reference standards of sediments (e.g., BCR-2, SGR-1b, RGM-2 and DGH). The accuracy of measurement is better than 2–5% and precision <2. EDS reports of the investigated coprolites are provided as Supplementary Data S1. The specimens and slides relating to the coprolite specimens investigated herein are housed at BSIP, Lucknow, India (BSIP locality no. 10145; Specimens nos. BSIP 42253-42282; Museum slide nos. 17250-17251).

## **RESULTS**

### *Morphological Characterization*

A total of fourteen coprolite specimens [specimen nos. LTK/2101-154 (BSIP 42254), LTK/2101-234 (BSIP 42255), VVK/BNP/GEO2 (BSIP 42256), VVK/BNP/GEO1 (BSIP 42253), LTK/2101-194 (BSIP 42258), LTK/2101-351 (BSIP 42260), VVK/BNP/GEO12 (BSIP 42257), LTK/2101-321 (BSIP 42261), LTK/2101-14 (BSIP 42259), LTK/2101-88 (BSIP 42262), LTK/2101-21 (BSIP 42263), LTK/2101-15 (BSIP 42265), VVK/BNP/GEO9 (BSIP 42264), VVK/BNP/GEO10 (BSIP 42266)] representing five morphotypes (M1-M5) are described in the present investigation (Figs. 2-3). It should be noted that the investigated coprolites specimens were recovered in association with vertebrates including fishes (mainly scales including those belonging to the genus *Lepisosteus indicus*), chelonians (carapace fragments and vertebrae), and crocodilians (scutes and isolated teeth) (Fig. 4).

*Morphotype M1:* Four coprolite specimens [specimen nos. VVK/BNP/GEO1 (BSIP 42253), LTK/2101-154 (BSIP 42254), LTK/2101-234 (BSIP 42255), VVK/BNP/GEO2 (BSIP 42256)] represent morphotype *M1* (Figs 2a-d). The morphotype *M1* depicts whitish to pale yellow colouration, with an average length of 26.46 mm and an average width of 23.17 mm (refer to Table 1), spherical with rounded to sub-rounded outline (length/width ranging from 0.92 mm to 1.25 mm; Table 1), are circular/sub-circular in cross-section, with external surface generally smooth that may possess a few pits and/or desiccation cracks, depict biotic inclusions consisting of both plant remains and partially digested bone content (refer to section 'Abiotic and biotic inclusions') and are chemically phosphatic (refer to section 'XRD and XRF analyses').

*Remarks:* This is the first record of large (cm-sized) spherical (with rounded to sub-rounded outline) coprolites from India i.e., morphotype *M1* is morphologically different from the previously known Mesozoic-Cenozoic coprolites from India (refer to Kapur et al. 2020). Global records suggest that spherical-shaped coprolites (with rounded to sub-rounded outlines) have been earlier recorded from the Lower Triassic limestone unit (part of the

Lower Gogolin Beds representing a shallow-water coastal palaeodepositional environment) in a quarry section, Upper Silesia, southern Poland (refer to Fig. 4B in Brachaniec et al. 2015). The coprolites recorded by Brachaniec et al. (2015) have been linked to sauropterygian reptiles based on the presence of vertebrate remains (as inclusions) and associated faunal remains. Further, the spherical coprolites (see Brachaniec et al. 2015) are at least 2 times smaller (being ~1 cm in diameter) compared to the morphotype M1 recorded herein. Upper Triassic (Rhaetian) lacustrine mudstone unit belonging to the Kap Stewart Formation, East Greenland is also known to yield somewhat spherical-shaped coprolites (see Figs. 4d-g in Hansen et al. 2015) that preserve bone material (thus linked to unidentified carnivore) and approximately 50% smaller than morphotype M1 recorded from Lotkheri locale. Lucas et al. (2012) previously recorded ‘rounded’ (however, in polar view) coprolites (tentatively assigned to *Alococopros triassicus*) from the late Eocene marginally lacustrine sandy shale unit along the Aksyir River, Zaysan Basin, Kazakhstan. However, *Alococopros triassicus* recorded from Zaysan Basin differs from morphotype M1 in being smaller (length ~16-23 mm; maximum diameter 9-16 mm) and having longitudinal striations. Recently, Muftah et al. (2020) recorded spherical coprolites from the Neogene (late Miocene) Sahabi Formation (Sirt Basin, Libya) that are smaller in size (i.e., diameter ranging from 14 mm to 19.5 mm) in comparison to morphotype M1 recorded in our study. Spherical scats are known to be produced by extant gharials (*Gavialis gangeticus*) that are quite similar in size (~20 mm in diameter) to the coprolite morphotype M1 recorded in the present investigation (see Milàn 2012). However, the presence of biotic inclusions in the form of both plant and undigested bone matter within morphotype M1 coprolites (refer to section ‘Biotic and abiotic inclusions’, this study) suggests that morphotype M1 were most likely produced by omnivorous chelonians as opposed to exclusively carnivorous crocodiles (for details refer to section ‘Discussion’).



*Morphotype M2:* This morphotype is represented by the five specimens: VVK/BNP/GEO12 (BSIP 42257), LTK/2101-194 (BSIP 42258), LTK/2101-351 (BSIP 42260), LTK/2101-321 (BSIP 42261)(Figs 2e-i) that are whitish to pale yellow coloured, with an average length of 25.53 mm and an average width of 26.03 mm (refer to Table 1), tear-drop shaped (with length/width ranging from 0.61 mm to 1.46 mm; Table 1), anisopolar with one end slightly tapered/arched due to a conspicuous inclination along its longitudinal axis on one side, elliptical in cross-section, external surface generally smooth that may possess pits and/or desiccation cracks, showcase biotic inclusions consisting of both plant remains, partially digested bone content (refer to section '*Biotic and abiotic inclusions*') and phosphatic in chemical nature (refer to section '*XRD & XRF analyses*').

*Remarks:* This is one of the most common morphotype observed at the Lotkheri locale (Figs 2e-i) and was previously illustrated by Kapur et al. (2006). Kapur et al. (2006) linked the recovered coprolites (single morphotype) to Archosauria due to the associated presence of vertebrate remains of both crocodiles and turtles [refer to Plate 1 (Fig. 26) in Kapur et al. 2006]. However, the author did not attempt to analyse the Lotkheri coprolites for biotic-abiotic inclusions and/or geochemically. Apart from the Lotkheri locale, published records from India suggest that the teardrop-shaped anisopolar (one end slightly tapered/arched due to a conspicuous inclination along its longitudinal axis on one side) coprolites have not been recorded previously from the Mesozoic [particularly from the Maastrichtian infratrappean (Lameta Formation) deposits at Pisdura locale, central India (see Matley 1939)]. We observe a slight morphological resemblance of morphotype M2 with coprolites assigned to 'Group 2 (Type A) Morphotype' by Sharma and Patnaik (2010) from the Miocene Baripada beds of Orissa, India (refer to Fig. 2b in Sharma and Patnaik 2010). These authors also recorded a 'Tear-Drop shaped' coprolite (linked to crocodiles) that measures 2.1 cm in diameter (refer to Fig. 2a in Sharma and Patnaik 2010); however, the illustrated specimen is broken to allow

comparison with morphotype M2 coprolites reported in our study. Inclusions of both plant and bone matter within morphotype M2 coprolites (refer to section '*Biotic and abiotic inclusions*') hint at an omnivorous producer that is most likely chelonians (as detailed in section '*Discussion*'). Interestingly, a few specimens assigned to morphotype M2 showcase bite marks on the external surface (Figs. 2g, 2i1) that we herein link to the garfish genus *Lepisosteus* (for details refer to section '*Discussion*'). Global records exist on Upper Cretaceous vertebrate coprolites (Waldman 1970; Broughton et al. 1978; Nobre et al. 2008; Hollocher et al. 2010; Suoto 2010; Hunt et al. 2012, 2015; Sullivan & Jasinski 2012; Suozo et al. 2012; Godfrey & Palmer 2015; Milán et al. 2015; Schwimmer et al. 2015; Brachaniec & Wieczorek 2016; Segesdi et al. 2017); however, none of these are morphologically comparable to morphotype M2 recorded in the present investigation.

**Morphotype M3:** Morphotype M3 is represented by the following specimens: LTK/2101-88 (BSIP 42262), and LTK/2101-21 (BSIP 42263) (Figs. 3a1-a2, b1-b3). Morphotype M3 coprolites are generally whitish to pale yellow coloured, elliptical with an average length measuring 29.71 mm and average width measuring 22.58 mm (Table 1), anisopolar, display constrictions, with burrows/pits and/or desiccation cracks generally observed on the external surface, and geochemically calcium phosphatic.

**Remarks:** Coprolites morphologically similar to Morphotype 3 (recorded herein) have not been reported previously from the Mesozoic (e.g., Jurassic Kota Formation, Triassic Maleri Formation, Maastrichtian infra- and intertrappean sediments) and the Cenozoic (Lutetian Harudi Formation, Aquitanian Khari Nadi Formation, Burdigalian-Langhian Chassra Formation, and the Burdigalian Baripada beds) time intervals of India. The presence of biotic inclusions in the form of both plant and undigested bone matter within morphotype M3 coprolites (refer to section '*Biotic and abiotic inclusions*') suggests that morphotype M3 were most likely produced by omnivorous chelonians as opposed to exclusively carnivorous

crocodiles (for details refer to section '*Discussion*'). Reptilian coprolites within the size range of Morphotype 3 (this study) are well-known to occur within the Upper Cretaceous sedimentary succession across the globe (Waldman 1970; Broughton et al. 1978; Nobre et al. 2008; Hollocher et al. 2010; Suoto 2010; Hunt et al. 2012, 2015; Sullivan & Jasinski 2012; Suozo et al. 2012; Godfrey & Palmer 2015; Milán et al. 2015; Schwimmer et al. 2015; Brachaniec & Wieczorek 2016; Segesdi et al. 2017); however, they do not compare in general shape depicted by Morphotype 3.

*Morphotype 4:* We herein assign specimen nos. LTK/2101-15 (BSIP 42265), and VVK/BNP/GEO9 (BSIP 42264) to Morphotype 4 (Figs.3c1-c2, d). Morphotype 4 coprolites display pale yellow to reddish brown colouration, cylindrical but curved along the longitudinal axis, average length measuring 40.42 mm, average width measuring 30.93 mm (Table 1), having burrows/pits and/or desiccation cracks on the external surface, and calcium phosphatic in chemical nature.

*Remarks:* Thin sections of the Morphotype 4 coprolites (refer to section '*Biotic and abiotic inclusions*') suggests that these ichnofossils were most likely produced by crocodiles rather than chelonians (for details refer to section '*Discussion*'). Coprolite records from India suggest that the ichnofossils linked to crocodiles have been recorded previously from the Lutetian Harudi Formation, Kachchh region, western India [refer to Plate II (Figs.7-8) in Sahni and Mishra 1975]; however, incomplete nature of specimen nos. LTK/2101-15 (BSIP 42265) and VVK/BNP/GEO9 (BSIP 42264) do not allow direct comparisons with Harudi coprolites, at this stage. A common occurrence of coprolites linked to crocodiles within the Upper Cretaceous sedimentary succession of the globe has been observed in the published literature (Hunt et al. 2012, 2015 and references therein); however, due to fragmentary nature of specimens assigned to Morphotype 4, direct comparisons are not possible at this stage.

*Morphotype 5:* This morphotype is represented by a single complete specimen VVK/BNP/GEO10 (BSIP 42266) (Figs. 3e1-e2). Morphotype 5 displays a pale yellowish white colouration, irregularly folded, measuring 36.66 mm in length and 13.33 mm in width (Table 1), anisopolar with both ends pinched and tapered, displaying constrictions forming conspicuous lobes and having desiccation cracks on the external surface(Figs. 3e1-e2).

*Remarks:* The specimen VVK/BNP/GEO10 (BSIP 42266) has not been analysed for biotic-abiotic inclusions through thin section techniques and/or analysed chemically. A separate detailed investigation utilizing the non-destructive micro-CT analysis is underway to link the specimen VVK/BNP/GEO10 (BSIP 42266) to its producer. However, the presence of constrictions that form conspicuous lobes strongly points towards an organic origin (refer to Hantzschel et al. 1968; Broughton et al. 1978). Further, the common presence of crocodilian and chelonian remains at Lotkheri (Fig. 4) suggests that Morphotype 5 was most likely produced by a reptilian. Interestingly, none of the previously recorded coprolite morphotypes or ichnotaxa recorded within the Mesozoic-Cenozoic sediments of India is comparable to Morphotype 5. In terms of global records on coprolites, irregularly folded coprolites recorded from the late Cretaceous Whitemud Formation, Canada [refer to Plate 43 (Fig. 18) Broughton et al., 1978] are morphology quite comparable to the Morphotype 5 (this study); however, the Canadian coprolites either display longitudinal striations or polygonal cracks on their external surfaces unlike Morphotype 5 from Lotkheri, central India. Amstutz (1958) recorded four coprolite specimens from the ‘Tertiary’ sediments of Salmon Creek, Washington, USA. Of these, one of the unnamed morphotype specimens is almost identical to Morphotype 5, recorded herein. However, the coprolite record by Amstutz (1958) may be doubted due to chemical analysis showing iron being the major chemical component of the specimen with a complete absence of phosphorous (refer to pp.11-12 in Hantzschel et al. 1968). An irregular morphotype “Ichnotaxon I” represented by a single specimen (that displays the presence of

three lobes on the outer surface with desiccation cracks) from the Late Miocene of Egypt [refer to Plate II (Fig.5) in Muftah et al. 2020] is quite comparable to Morphotype 5 from Lotkheri. However, “Ichnotaxon I” of Muftah et al. (2020) is at least two times larger than specimen no. VVK/BNP/GEO10 (BSIP 42266).

### *Biotic and abiotic inclusions*

It should be noted that the present investigation reveals for the first time the internal texture, abiotic and biotic inclusions within a collection of vertebrate coprolites from a Maastrichtian intertrappean deposit in India (i.e., Lotkheri) utilizing both scanning electron microscopy (Figs. 5-6) and digital scanning of thin sections (Fig. 7). We observe the presence of micron-sized porous structures (or ‘vesicles’), and walled egg-like mineral spheres (or ‘microspherulites’) (Figs. 6e-f) within the investigated coprolites. The observed porous structures are generally considered as a reminiscence of escaping gases during the process of decomposition of the faecal matter (Lamboy et al. 1994; PurnachandraRao & Lamboy 1995; Northwood 2005; Kapur et al. 2020; Sagar et al. 2022). The microspherulites (i.e., egg-like mineral spheres) are commonly ascribed to mineral pseudomorphs of sulphur-producing bacteria (Hollocher et al. 2010; Owocki et al. 2013; Bajdek et al. 2016; Kapur et al. 2020; Sagar et al. 2022). Additional biotic remains observed within the Lotkheri coprolites include remains of freshwater sponge spicule morphotype *Acanthoxea* (Fig. 7c, 7g), possible dung beetle eggs (Figs. 7d-e) and some burrow structures (Fig. 7i) (also refer to section ‘*Discussion*’).

SEM analyses show the dominant presence of phosphatic (Hydroxyapatite - HAP) crystals (Figs. 6, 8) in the coprolite morphotypes recorded herein. The multi-spot EDS examination of the HAP crystals indicates a high concentration of Ca, P, and O. Interestingly, the HAP crystals showcase three distinct morphologies: spherical (HAP-S), rod-like (HAP-R), and needle-like (HAP-N) (Figs. 6, 8) (also refer to section ‘*Discussion*’).

## *XRD and XRF analyses*

Bulk mineralogical data based on the XRD results show that the eight analysed coprolite specimens are dominantly comprised of Hydroxyapatite apart from the presence of other accessory minerals such as Barite, Quartz and Feldspar (Fig. 9a-b). However, XRD data on the lithological samples suggest the minerals Feldspar, Quartz, and Plagioclase occur in a decreasing order of preponderance in terms of percentage (Fig. 9c). Additionally, the minerals Feldspar, Quartz, and Plagioclase within the coprolite-yielding host-lithology sample LTK-2 are present in lesser proportion compared to that in the unfossiliferous sample LTK-1 (Fig. 9c). Considering the XRF data on major oxides the relative composition (in %) concerning  $\text{SiO}_2$ ,  $\text{Al}_2\text{O}_3$ ,  $\text{Fe}_2\text{O}_3$ ,  $\text{Na}_2\text{O}$ , and  $\text{K}_2\text{O}$  within sample LTK-1 is less as compared to that in coprolite-yielding sample LTK-2 (Fig. 9d). This observation is also substantiated by the mineral composition shown in the XRD spectra. Further, the enrichment of  $\text{SiO}_2$  and  $\text{Fe}_2\text{O}_3$  in the sample LTK-1 indicates more sediment-water interaction that may have been unfavourable for coprolite preservation within LTK-1 sediments. In contrast, the sample LTK-2 showcasing a relatively high percentage of  $\text{SiO}_2$ ,  $\text{Al}_2\text{O}_3$ ,  $\text{Na}_2\text{O}$ , and  $\text{K}_2\text{O}$  favours the preservation of fossils including the coprolites recorded herein. Geochemical data corroborate field and laboratory palaeontological efforts carried out on the unfossiliferous red clay sample LTK-1 and fossiliferous (coprolite and vertebrate yielding) grey clay sample LTK-2.

## **DISCUSSION**

Reptilian coprolites from the Maastrichtian intertrappean deposit of Lotkheri (central India) reveal the presence of five morphotypes (i.e., spherical-M1, tear-drop shaped-M2, elliptical-M3, cylindrical-M4 and irregularly folded-M5) based on their geometry, surface, and internal textures. The common presence of undigested bone matter (Figs. 5a1, 5b1, 5c1, 5d, 5e1) including the presence of fish scales (Figs. 7a-b) apart from plant remains (Fig. 7f, 7h) within a few investigated coprolites (mainly within morphotypes M1, M2, M3) supports an

omnivorous diet of the producer. Several extant chelonians species belonging to the family Trionychidae (i.e., *Amydacartilaginea*, *Nilssonia gangeticus* (= *Aspideretes gangeticus*), *Nilssoniahurum* (= *Aspidereteshurum*), *Trionyxtriunguis*) that generally dwell in freshwater ponds and/or rivers have been documented to consume an omnivorous diet (Jensen & Das 2008 and references therein). Recovery of chelonian remains (Figs. 4a-b) in association with the coprolites (recorded herein) further supports our inference that the producers of morphotypes M1-M3 were chelonians (also refer to section “*Morphological characterization*”). The absence of bone matter within morphotype M4 coprolite specimen LTK/2101-15 (BSIP 42265) suggests that the producer animal had an effective digestive system compared to chelonians. Extant crocodiles are known to have an effective digestive system (i.e., having stomach acid with a pH value up to ~2 and in a volume quite higher compared to other carnivores in the animal kingdom) to allow complete digestion of vertebrate remains (Fisher 1981; Coulson et al. 1989; Trutnau & Sommerlad 2006; Balaguera-Reina et al. 2018 and references therein). In a separate study on modern crocodilians, Milàn (2012) observed a complete absence of skeletal remains in the scats of crocodiles that were provided with a diet comprising of piglets, fish and chicken. Numerous crocodilian elements in the form of scutes and isolated teeth (Figs. 4c-l) were recovered from Lotkheri intertrappean deposits in association with coprolites during the present investigation (also refer to Kapur et al. 2006). Thus, it is quite likely that crocodiles are the producers of the morphotype M4 coprolites. Due to the reasons mentioned earlier, Morphotype 5 specimen no. VVK/BNP/GEO10 (BSIP 42266) was excluded from the destructive analyses; however, its morphology and associated faunal remains hint at a reptilian producer. Additional, biotic inclusions observed within the Lotkheri coprolites include remains of freshwater sponge spicule morphotype *Acanthoxea*, possible dung beetle eggs and some backfilled burrow structures. Fresh water sponge spicules (in particular, morphotype *Acanthoxea*) have been

previously recorded within the Maastrichtian Type-A coprolites (linked to titanosaurid sauropods) from the infratrappean (Lameta Formation) deposits of Pisdura, central India (Khosla et al. 2015) and recently within the Miocene chelonian coprolites from Kachchh region, western India (Sagar et al. 2022). Many extant dung beetle species (e.g., *Onthophagus gazella*) are known to form tunnels/burrows structures to sustain brood chambers (Chin and Gill 1996 and references therein). It is observed that the pattern and size of the burrows and brood chambers are unique to extant species of dung beetles; however, it is difficult to link these inclusive structures to a particular taxon in the case of deep-time fossilized faecal matter i.e., coprolites (Chin & Gill 1996 and references therein). The presence of burrow structures, dung beetle eggs, and soft parts of beetles within coprolites are not uncommon in the fossil record and provide unique palaeoenvironmental-palaeoecological data (Qvarnström et al. 2016, 2017, 2021 and references therein). In the past few years, the non-destructive synchrotron microtomography technique has proven to be quite useful to identify dung beetle elements within coprolites (Qvarnström et al. 2021 and references therein). As already mentioned, non-destructive techniques have not been utilized in the present investigation to identify biotic inclusions within Lotkheri coprolites and hint at the scope of future investigations on Mesozoic-Cenozoic coprolite material from India. However, it is generally agreed that the presence of burrow and/or egg-like structures within coprolites linked to dung beetle are suggestive of the prevalence of a terrestrial palaeoenvironment. Associated faunal remains support that the Lotkheri coprolites were deposited in a palustrine/lacustrine fresh to brackish water environment.

Rare occurrences of external markings on coprolites such as feeding traces or tooth impressions have been recorded in the published literature that has been linked to tiger sharks (e.g., genus *Galeocerdo*) or gar fishes (e.g., genus *Lepisosteus*) (refer to Figs. 3I, 5I in Månsby 2009; Fig. 2A in Godfrey & Smith 2010; Figs. 1-3 in Godfrey & Palmer 2015).



Bite marks are observed on the external surface of a few Lotkheri coprolite specimens assigned to morphotype M2 (Figs. 2g, 2i1). The glancing bite approximately 2 cm in length (Fig. 2g) is identical to the one assigned to the garfish genus *Lepisosteus* by Godfrey & Palmer (2015) while smaller (<5 mm length) 3-paired (nearly conjoined at one end) troughs (Fig. 2i1) are identical to the one recorded by these workers but assigned to an unknown animal. Interestingly, fish scales belonging to *Lepisosteus indicus* (Figs. 4n-p) were also recovered in association with the coprolite assemblage recorded herein and argues in favour of the glancing bite produced by this fish during coprophagy.

The phosphatic composition of the coprolites recorded herein is confirmed by utilizing scanning electron microscopy and geochemical data. Interestingly, the Hydroxyapatite (HAP) crystals observed as inclusions depict three distinct morphologies: spherical (HAP-S), rod-like (HAP-R), and needle-like (HAP-N). We envisage that the freshly excreted faecal matter that consisted of an ionic aqueous solution containing different ions such as  $\text{Ca}^{2+}$ ,  $\text{PO}_4^{3-}$ ,  $\text{OH}^-$ , and  $\text{H}^+$  help explain the formation of these varied types of phosphatic crystals (Fig10). The growth unit model as shown in Fig. 10 postulates that the presence of  $\text{Ca}^{2+}$ ,  $\text{PO}_4^{3-}$ , and  $\text{H}^+/\text{OH}^-$  ions in newly expelled faeces constitutes the growth unit, and the pH regulates the concentration of both positively and negatively charged growth units. Neutral conditions are crucial for the concentration of positive and negative growth units to balance, leading to the crystallization and maturation of HAP crystals through various morphologies. A pH of around 7-8 in the post-depositional environment remineralizes faeces into HAP, which is the least soluble phase formed under neutral or basic conditions. Overall, calcium phosphate in coprolite is a result of both precipitation and adsorption processes, where minerals from the surrounding soil or water can deposit on its surface or adsorb onto it. The crystalline structures, intermediate forms, and amorphous aggregates of calcium phosphate in coprolites provide valuable information about the organism's gut and the events that influenced calcium

phosphate precipitation before, during, and after its formation. Additionally, organic matter in faeces can serve as a template for calcium phosphate precipitation, affecting its development. The remineralisation of calcium phosphate is dependent on various factors, including pH, concentration, temperature changes, and metabolic processes.

## **CONCLUSIONS**

A detailed account of reptilian coprolites from the Maastrichtian intertrappean deposit of Lotkheri (central India) reveals the presence of five morphotypes i.e., spherical-M1, tear-drop shaped-M2, elliptical-M3, cylindrical-M4 and irregularly folded-M5. The common presence of undigested bone matter and plant remains within morphotypes M1, M2, and M3 supports an omnivorous diet of the producer most likely chelonians. Absence of bone inclusions within morphotype M4 hints at a producer having an effective digestive system most likely a crocodilian. The occurrence of chelonian (mainly scutes) and crocodilian (scutes and teeth) remains in association with coprolites (recorded herein) supports the proposed reptilian producer associations. Scanning electron microscopy and geochemical data confirms the phosphatic composition of the reptilian coprolites investigated herein. Hydroxyapatite crystals (as inclusions) showcase three distinct morphologies i.e., spherical, rod-shaped, and needles. The proposed chemical model envisages that the freshly excreted faecal matter consisting of an ionic aqueous solution containing different ions such as  $\text{Ca}^{2+}$ ,  $\text{PO}_4^{3-}$ ,  $\text{OH}^-$ , and  $\text{H}^+$  explains the formation of these varied types of phosphatic crystals. The external surface of morphotype 2 coprolites provides rare evidence of two different types of bite marks herein linked to garfish *Lepisosteus* and to an unknown animal practising coprophagy. Data on inclusions (both biotic and abiotic), and associated vertebrate remains indicate that the recorded coprolite ichnofossils were deposited in a palustrine/lacustrine fresh to brackish water palaeoenvironment.

## ACKNOWLEDGEMENTS

The authors are thankful to the Director (BSIP, Lucknow) for providing the necessary infrastructure, encouragement, and permission(s) to carry out this investigation...

## REFERENCES

- Amstutz, G. C. (1958). Coprolites: a review of the literature and a study of specimens from southern Washington. *Journal of sedimentary research*, 28(4), 498–508.
- Bajdek, P., and Bienkowska-Wasiluk, M. (2020). Deep-sea ecosystem revealed by teleost fish coprolites from the Oligocene of Poland. *Palaeogeography Palaeoclimatology Palaeoecology*, 540, 109546. <https://doi.org/10.1016/j.palaeo.2019.109546>.
- Bajdek, P., Qvarnström, M., Qwocki, K., Sulej, T., Sennikov, A.G., Golubev, V.K., & Niedźwiedzki, G. (2016). Microbiota and food residues including possible evidence of premammalian hair in Upper Permian coprolites from Russia. *Lethaia*, 49, 455–477. <https://doi.org/10.1111/let.12156>
- Balaguera-Reina, S. A., Venegas-Anaya, M., Beltrán-López, V., Cristancho, A., & Densmore III, I. D. (2018). Food habits and ontogenetic dietary partitioning of American crocodiles in a tropical pacific island in central America. *Ecosphere*, 9(9), e02393. <https://doi.org/10.1002/ecs2.2393>.
- Barrios-de Pedro, S., Poyato-Ariza, F.J., Moratalla, J.J., & Buscalioni, Á.D. (2018). Exceptional coprolite association from the early cretaceous continental Lagerstätte of Las Hoyas, Cuenca, Spain. *PloS One*, 13, e0196982. <https://doi.org/10.1371/journal.pone.0196982>.
- Brachaniec, T., Niedźwiedzki, R., Surmik, D., Krzykowski, T., Szopa, K., Gorzelak, P., & Salamon, M.A. (2015). Coprolites of marine vertebrate predators from the lower Triassic of southern Poland. *Palaeogeography Palaeoclimatology Palaeoecology*, 435, 118–126. <https://doi.org/10.1016/j.palaeo.2015.06.005>.
- Brachaniec, T., & Wieczorek, A. (2016). Possible vertebrate coprolites from the upper cretaceous (coniacian) of the sudetes mountains (southern Poland). *Carnets de Géologie*, 16, 349–354. <https://doi.org/10.4267/2042/60665>.
- Broughton, P., Simpson, F., & Whitaker, S. (1978). Late cretaceous coprolites from western Canada. *Palaeontology*, 21, 443–453.
- Chin, K. (2002). Analyses of coprolites produced by carnivorous vertebrates. *The Paleontological Society Papers*, 8, 43–50. <https://doi.org/10.1017/s1089332600001042>.
- Chin, K., Feldmann, R.M., & Tashman, J.N. (2017). Consumption of crustaceans by megaherbivorous dinosaurs: dietary flexibility and dinosaur life history strategies. *Scientific Reports*, 7, 11163. <https://doi.org/10.1038/s41598-017-11538-w>.
- Chin, K., & Gill, B.D. (1996). Dinosaurs, dung beetles, and conifers: participants in a cretaceous food web. *Palaos*, 11(3), 280–285.
- Coulson, R. A., Herbert, J.D., & Coulson, T.D. (1989). Biochemistry and physiology of alligator metabolism in vivo. *American Zoologist*, 29(3), 921–934.
- Dentzien-Dias, P., Carrillo-Briceño, J.D., Francischini, H., & Sánchez, R. (2018). Paleoeological and taphonomical aspects of the late Miocene vertebrate coprolites (Urumaco formation) of Venezuela. *Palaeogeography Palaeoclimatology Palaeoecology*, 490, 590–603. <https://doi.org/10.1016/j.palaeo.2017.11.048>.

- Fantasia, A., Adatte, T., Spangenberg, J.E., & Font, E. (2016). Palaeoenvironmental changes associated with deccan volcanism, examples from terrestrial deposits from central India. *Palaeogeography Palaeoclimatology Palaeoecology*, 441, 165–180. <https://doi.org/10.1016/j.palaeo.2015.06.032>.
- Gates-Rector, S., & Blanton, T. (2019). The powder diffraction file: a quality materials characterisation database. *Powder Diffraction*, 32(4), 352–360.
- Godfrey, S., & Palmer, B. (2015). Gar-bitten coprolite from South Carolina, USA. *Ichnos*, 22, 103–108.
- Godfrey, S., & Smith, J.B. (2010). Shark bitten vertebrate coprolites from the Miocene of Maryland. *Naturwissenschaften*, 97, 461–467.
- Hansen, B., Milan, J., Clemmensen, L., Adolfsson, J., Estrup, E., Klein, N., Mateus, O., & Wings, O. (2015). Coprolites from the late Triassic KapStewart Formation, Jameson Land, East Greenland: morphology, classification and prey inclusions. *Geological Society, London, Special Publications*, 434. <http://doi.org/10.1144/sp434.12>.
- Häntzschel, W., El-Baz, F., & Amstutz, G.C. (1968). Coprolites: an annotated bibliography. *Memoirs of the Geological Society of America*, 108, 1–132.
- Hollocher, K.T., Hollocher, T.C., & Rigby, J.K. (2010). A phosphatic coprolite lacking diagenetic permineralization from the Upper Cretaceous Hell Creek Formation, northeastern Montana: importance of dietary calcium phosphate in preservation. *Palaios*, 25, 132–140. <https://doi.org/10.2110/palo.2008.p08-132r>.
- Hunt A.P., Lucas S.G., & Spielmann J.A. (2012). The vertebrate coprolite collection at the Natural History Museum (London). In A.P. Hunt, J. Milàn, S.G. Lucas, & J.A. Spielmann (Eds.), *Vertebrate Coprolites: New Mexico Museum of Natural History and Science Bulletin*, 57, 125–130.
- Hunt, A., Lucas, S.G., Milàn, J., Lichtig, A.J., & Jagt, J.W.M. (2015). Vertebrate coprolites from cretaceous chalk in Europe and north America and the shark surplus paradox. In R.M. Sullivan & S.G. Lucas (Eds.), *Fossil record 4: New Mexico Museum of Natural History and Science Bulletin*, 67, 63–68.
- Jensen, K., & Das, I. (2008). Cultural exploitation of freshwater turtles in Sarawak, Malaysian Borneo. *Chelonian conservation biology*, 7, 281–285. <https://doi.org/10.2744/ccb-0657.1>.
- Kapur, V.V., Bajpai, S., Sarvanan, N., & Das, D.P. (2006). Vertebrate fauna from Deccan intertrappean beds of Bhanpura, Mandsaur District, Madhya Pradesh. *Gondwana Geological Magazine*, 21, 43–46.
- Kapur, V.V., & Khosla, A. (2019). Faunal elements from the deccan volcano-sedimentary sequences of India: a reappraisal of biostratigraphic, palaeoecologic, and palaeobiogeographic aspects. *Geological journal*, 54, 2797–2828. <https://doi.org/10.1002/gj.3379>.
- Kapur, V.V., Kumar, K., Morthekai, P., & Chaddha, A.S. 2020. Palaeodiet of Miocene producers and depositional environments: inferences from the first evidence of microcoprolites from India. *Acta Geologica Sinica – English Edition*, 94, 1574–1590. <https://doi.org/10.1111/1755-6724.14293>.
- Keller, G., Paula, M., Johannes, M., Nicolas, T., Jahanavi, P., Jorge, S., Sigal, A., & Sarit, A.P. (2020). Mercury linked to deccan trap volcanism, climate change and the end-Cretaceous mass extinction. *Global and Planetary change*, 194, 103312. <https://doi.org/10.1016/j.gloplacha.2020.103312>.
- Khosla, A., Chin, K., Alimohammadin, H., & Dutta, D. (2015). Ostracods, plant tissues, and other inclusions in coprolites from the late Cretaceous Lameta Formation at Pisdura, India: taphonomical and palaeoecological implications. *Palaeogeography Palaeoclimatology Palaeoecology*, 418, 90–100.

- 543 <https://doi.org/10.1016/j.palaeo.2014.11.003>.
- 544 Lamboy, M., Purnachandrarao, V., Ahmed, E., &Azzouzi, N. (1994). Nanostructure and  
545 significance of fish coprolites in phosphorites. *Marine Geology*, 120, 373–383.
- 546 Lucas, S.G., Spielmann, J.A., Hunt, A.P., &Emry, R.J. (2012). Crocodylian coprolites from  
547 the Eocene of the ZaysanBasin, Kazakstan. In A.P. Hunt, J. Milàn, S.G. Lucas, &J.A.  
548 Spielmann (Eds.), *Vertebrate Coprolites: New Mexico Museum of Natural History and*  
549 *Science Bulletin*, 57, 319–324.
- 550 Matley, C.A. (1939). The coprolites of Pisdura, central province. *Records of the Geological*  
551 *Survey of India*, 74, 535–547.
- 552 Månsby, U. (2009). Late cretaceous coprolites from the Kristianstad Basin, southern Sweden.  
553 Unpublished Bachelor Thesis, Department of Geology, Lund University, 16 pp.
- 554 Milàn, J.(2012). Crocodylian scatology – a look into morphology, internal architecture, inter-  
555 and intraspecific variation and prey remains in extant crocodylian feces. In A.P. Hunt,  
556 J. Milàn, S.G. Lucas, &J.A. Spielmann (Eds.), *Vertebrate Coprolites: New Mexico*  
557 *Museum of Natural History and Science Bulletin*, 57, pp. 65–72.
- 558 Milàn, J., Hunt, A., Adolfssen, J., Rasmussen, B., and Bjerager, M. (2015). First record of a  
559 vertebrate coprolite from the Upper Cretaceous (Maastrichtian) Chalk of StevnsKlint,  
560 Denmark. In R.M. Sullivan& S.G. Lucas (Eds.), *Fossil record 4: New Mexico Museum*  
561 *of Natural History and Science Bulletin*, 67, 227–230.
- 562 Muftah, A.M., El-Shawaihdi, M.H., Al Riay, M.H., &Boaz, N.T.(2020). Coprolites from the  
563 Neogene Sahabi Formation, northeasternSirtBasin of Libya. *Arabian Journal of*  
564 *Geosciences*, 13, 223. <https://doi.org/10.1007/s12517-020-5219-x>.
- 565 Nobre, P. H., De Souza Carvalho, I., De Vasconcellos, F. M., &Souto, P. R. (2008). Feeding  
566 behavior of the gondwaniccrocodylomorpha*Mariliasuchusamarali* from the Upper  
567 Cretaceous Bauru Basin, Brazil. *Gondwana Research*, 13, 139–  
568 145.<https://doi.org/10.1016/j.gr.2007.08.002>.
- 569 Northwood, C. (2005). Early Triassic coprolites from Australia and their  
570 palaeobiologicalsignificance. *Palaeontology*, 48, 49–68.  
571 <https://doi.org/10.1111/j.1475-4983.2004.00432.x>.
- 572 Owocki, K., Niedzwiedzki, G., Sennikov, A.G., Golubev, V.K., Janiszewska, K., &Sulej, T.  
573 (2013). Upper Permian vertebrate coprolites from Vyazniki and Gorokhovets, Vyatkian  
574 regional Stage, Russian platform. *Palaaios*, 27, 867–877.  
575 <https://doi.org/10.2110/palo.2012.p12-017r>.
- 576 Pande, K. (2002). Age and duration of the deccan traps, India: a review of radiometric and  
577 paleomagnetic constraints. *Journal of Earth System Science*, 111, 115–123.
- 578 Prasad, V., Strömberg, C.A.E., Alimohammadian, H., & Sahni, A. (2005). Dinosaur  
579 coprolites and the early evolution of grasses and grazers. *Science*, 310, 1177–1180.  
580 <https://doi.org/10.1126/science.1118806>.
- 581 Purnachandrarao, V., & Lamboy, M. (1995). Phosphorites from the Oman margin, ODP leg  
582 117. *OceanologicaActa*, 18, 289–307.
- 583 Qvarnström, M., Niedzwiedzki, G., &Žigaite, Ž.(2016). Vertebrate coprolites (fossilized  
584 faeces): an unexplored Konservat-Lagersätte. *Earth Science Reviews*, 162, 44–57.
- 585 Qvarnström, M., Niedzwiedzki, G., Tafforeau, P., Žigaite, Ž., &Ahlberg, P.E. 2017.  
586 Synchrotron phase-contrast microtomography of coprolites generates novel  
587 palaeobiological data. *Scientific Reports*, 7, 2723. [https://doi.org/10.1038/s41598-017-](https://doi.org/10.1038/s41598-017-02893-9)  
588 [02893-9](https://doi.org/10.1038/s41598-017-02893-9).
- 589 Qvarnström, M., Fikáček, M., Wernström, J.V., Huld, S., Beutel, R.G., Arriaga-Varela, E.,  
590 Ahlberg, P.E., &Niedzwiedzki, G.(2021). Exceptionally preserved beetles in a Triassic  
591 coprolite of putative dinosauriform origin. *Current Biology*, 31, 3374–3381.

- 592 Richter, G., &Baszio, S. (2001a). Traces of a limnic food web in the Eocene Lake Messel —  
593 a preliminary report based on fish coprolite analyses. *Palaeogeography*  
594 *Palaeoclimatology Palaeoecology*, 166, 345–368.<https://doi.org/10.1016/s0031->  
595 0182(00)00218-2.
- 596 Richter, G. &Baszio, S. (2001b). First proof of planctivory/insectivory in a fossil fish:  
597 *Thaumaturus intermedius* from the Eocene Lake Messel (FRG). *Palaeogeography*  
598 *Palaeoclimatology Palaeoecology*, 173, 75–85.  
599 [https://doi.org/10.1016/s0031-0182\(01\)00318-2](https://doi.org/10.1016/s0031-0182(01)00318-2).
- 600 Rummy, P., Halaclar, K., & Chen, H.(2021). The first record of exceptionally-preserved  
601 spiral coprolites from the Tsagan-TsabFormation (Lower Cretaceous), Tatal, western  
602 Mongolia. *Scientific Reports*, 11, 7891.<https://doi.org/10.1038/s41598-021-87090-5>.
- 603 Sagar, R., Kapur, V.V., Kumar, K., Morthekai, P., Sharma, A., Shukla, S., Ghosh, A.K.,  
604 Chauhan, G., & Thakkar, M.G. (2022). The first record on cm-sized vertebrate  
605 coprolites from the early-middle Miocene (Aquitania-Langhian) Khari Nadi and  
606 Chassra formations, Kutch Basin, western India: palaeobiological significance. *Pre-*  
607 *print SSRN electronic journal*.DOI: 10.2139/ssrn.4269941.
- 608 Sahni, A., &Mishra, V.P.(1975). Lower tertiary vertebrates from western India. *Monographs*  
609 *of the Palaeontological Society of India*, 3, 1–48.
- 610 Schoene, B., Samperton, K.M., Eddy, M.P., Keller, G., Adatte, T., Bowring, S.A., Khadri,  
611 S.F.R., &Gertsch, B.(2015). U-pb geochronology of the deccan traps and relation to the  
612 end-Cretaceous mass extinction. *Science*, 347(6218), 182–  
613 184.<https://doi.org/10.1126/science.aaa0118>.
- 614 Schwimmer, D., Weems, R., & Sanders, A. (2015). A late Cretaceous shark coprolite with  
615 baby freshwater turtle vertebrae inclusions. *Palaios*, 30, 707–713. DOI:  
616 10.2110/palo.2015.019.
- 617 Segesdi, M., Botfalvai, G., Bodor, E., Ósi, A., Buczkó, K., Dallos, Z., Tokai, R., &Földes, T.  
618 (2017). First report on vertebrate coprolites from the upper cretaceous (Santonian)  
619 CsehbányaFormation of Iharkút, Hungary. *Cretaceous Research*, 74, 87–  
620 99.<https://doi.org/10.1016/j.cretres.2017.02.010>.
- 621 Self, S., Jay, A., Widdowson, M., &Keszthelyi, L. (2008). Correlation of the deccan and  
622 Rajahmundry trap lavas: are these the longest and largest lava flows on earth?. *Journal*  
623 *of Volcanology and Geothermal Research*, 172, 3–19.  
624 <https://doi.org/10.1016/j.jvolgeores.2006.11.012>.
- 625 Sharma, M.K., & Patnaik, R. (2010). Coprolites from the lower Miocene Baripada beds of  
626 Orissa. *Current Science*, 99, 804–808.
- 627 Souto, P.R.F. (2010). Crocodylomorph coprolites from the Bauru basin, Upper Cretaceous,  
628 Brazil. *New Mexico Museum of Natural History and Science Bulletin*, 51, 201– 208.
- 629 Suazo, T.L., Cantrell, A.K, Lucas, S.G., Spielmann, J.A, & Hunt, A.P. (2012). Coprolites  
630 acrossCretaceous/Tertiary Boundary, San Juan Basin. In A.P. Hunt, J. Milàn, S.G.  
631 Lucas, &J.A. Spielmann (Eds.), *Vertebrate Coprolites: New Mexico Museum of*  
632 *Natural History and Science Bulletin*, 57,263–274.
- 633 Sullivan, R., &Jasinski, S. (2012). Coprolites from the Upper Cretaceous Fruitland, Kirtland  
634 and Ojo Alamo formations, San Juan Basin, New Mexico. In A.P. Hunt, J. Milàn, S.G.  
635 Lucas, &J.A. Spielmann (Eds.), *Vertebrate Coprolites: New Mexico Museum of*  
636 *Natural History and Science Bulletin*, 57, 255–262.
- 637 Trutnau, L. &Sommerlad, R. (2006). Crocodilians. Their natural history & captive  
638 husbandry, first ed. Chimaera, Frankfurt, Germany, 308–354 pp.
- 639 Vajda, V., Pesquero Fernández, M.D., Villanueva-Amadoz, U., Lehsten, V., andAlcalá,  
640 L.(2016). Dietary and environmental implications of early cretaceous predatory

- dinosaur coprolites from Teruel, Spain. *Palaeogeography Palaeoclimatology Palaeoecology*, 464, 134–142. <https://doi.org/10.1016/j.palaeo.2016.02.036>.
- Waldman, M. (1970). Comments on a cretaceous coprolite from Alberta, Canada. *Canadian Journal of Earth Sciences*, 7, 1008–1012.
- Yao, M., Sun, Z., Meng, Q., Li, J., & Jiang, D. (2022). Vertebrate coprolites from middle Triassic Chang 7 Member in Ordos Basin, China: palaeobiological and palaeoecological implications. *Palaeogeography Palaeoclimatology Palaeoecology*, 600, 111084. <https://doi.org/10.1016/j.palaeo.2022.111084>.
- Zatoń, M., Niedźwiedzki, G., Marynowski, L., Benzerara, K., Pott, C., Cosmidis, J., Krzykowski, T., & Filipiak, P. (2015). Coprolites of late Triassic carnivorous vertebrates from Poland: an integrative approach. *Palaeogeography Palaeoclimatology Palaeoecology*, 430, 21–46. <https://doi.org/10.1016/j.palaeo.2015.04.009>.

## EXPLANATION OF FIGURES

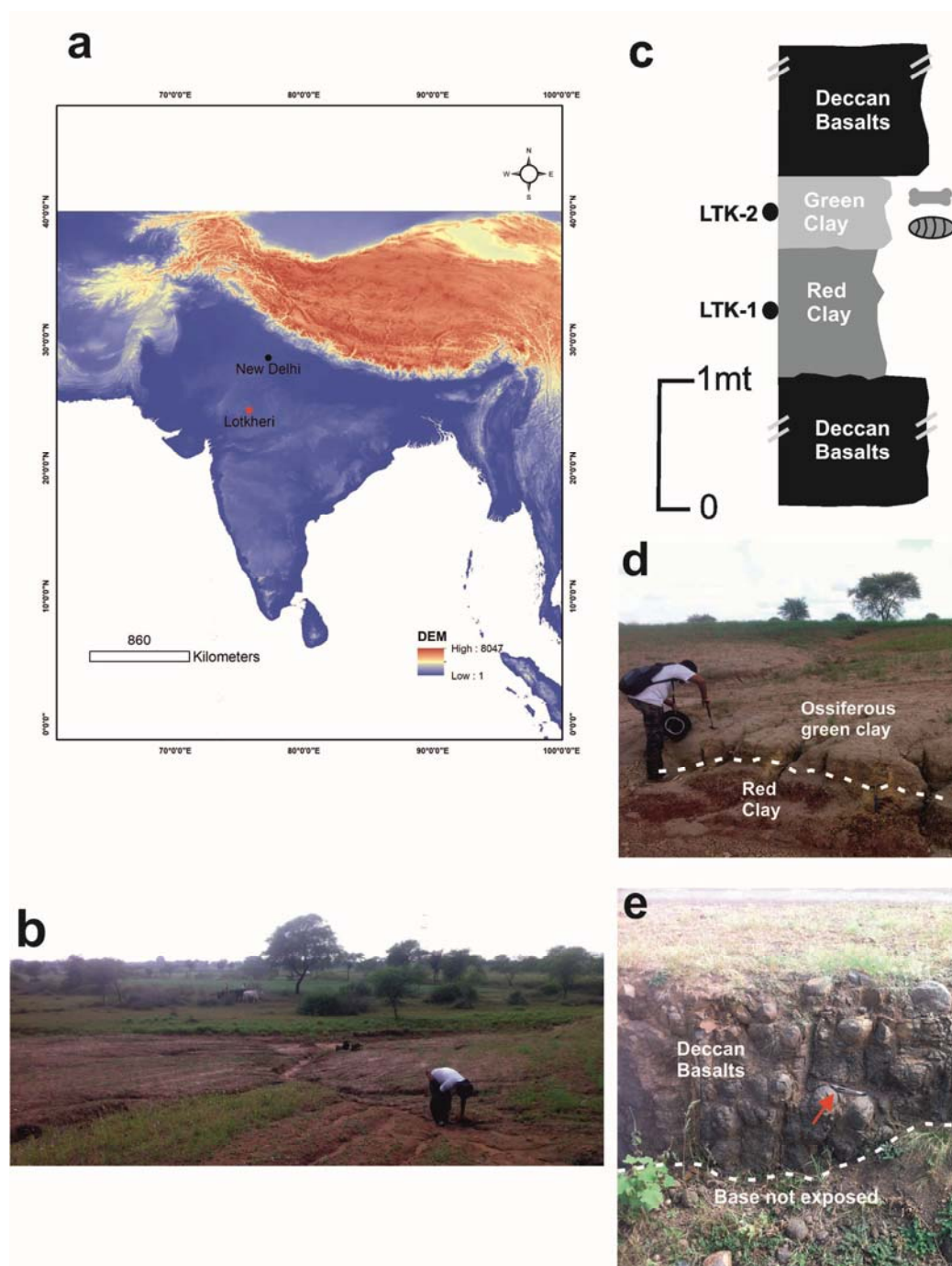


**Fig. 1.** (a) DEM map showing location of the investigated late Cretaceous (Maastrichtian) locale of Lotkheri in central India. (b) Panoramic view of the Lotkheri locale while conducting surface prospecting in the ploughed field (farmland) for vertebrate remains and associated coprolites. (c) Lithostratigraphic section. (d) Field photograph showing the contact between fossiliferous (coprolite-yielding) green clays and the underlying unfossiliferous red clays. (e) Exposure of the underlying basalt in a nala section in the vicinity of the coprolite-yielding locale showing spheroidal weathering, red arrow marks a pen for scale purposes.



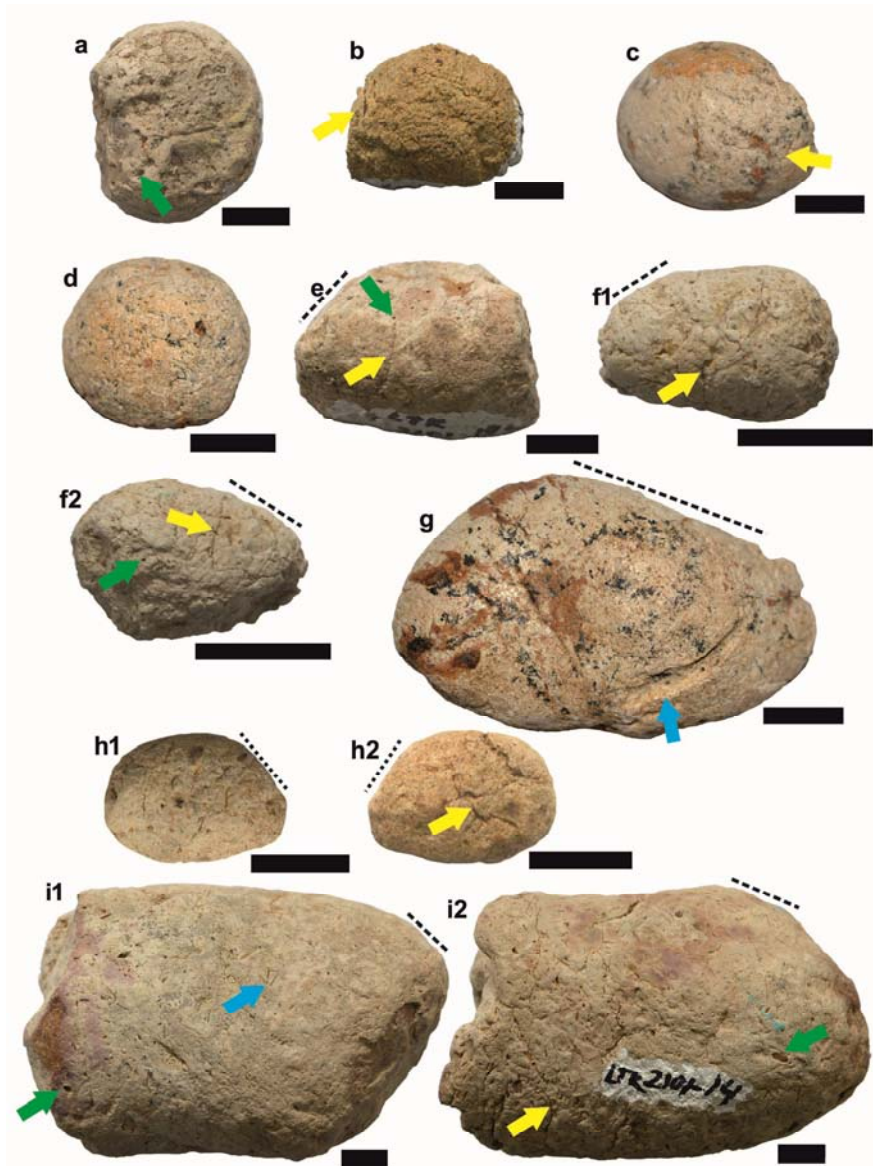


**Fig. 2.** Digital photographs of late Cretaceous (Maastrichtian) coprolite specimens recovered from the intertrappean deposit at Lotkheri, central India. (a-d) Spherical Morphotype M1, a. specimen no. LTK/2101-154 (BSIP 42254); b. specimen no. LTK/2101-234 (BSIP 42255); c. specimen no. VVK/BNP/GEO2 (BSIP 42256); d. specimen no. VVK/BNP/GEO1 (BSIP 42253). (e-i) Tear-drop shaped Morphotype M2, e. specimen no. LTK/2101-194 (BSIP 42258); f1-f2. specimen no. LTK/2101-351 (BSIP 42260); g. specimen no. VVK/BNP/GEO12 (BSIP 42257); h1-h2. specimen no. LTK/2101-321 (BSIP 42261); i1-i2. specimen no. LTK/2101-14 (BSIP 42259). Note: Green arrow marks burrow structures, yellow arrow marks desiccation cracks, light blue arrow points towards bite marks, and dashed lines highlight the conspicuous inclination. The scale bar equals 1 cm for all.

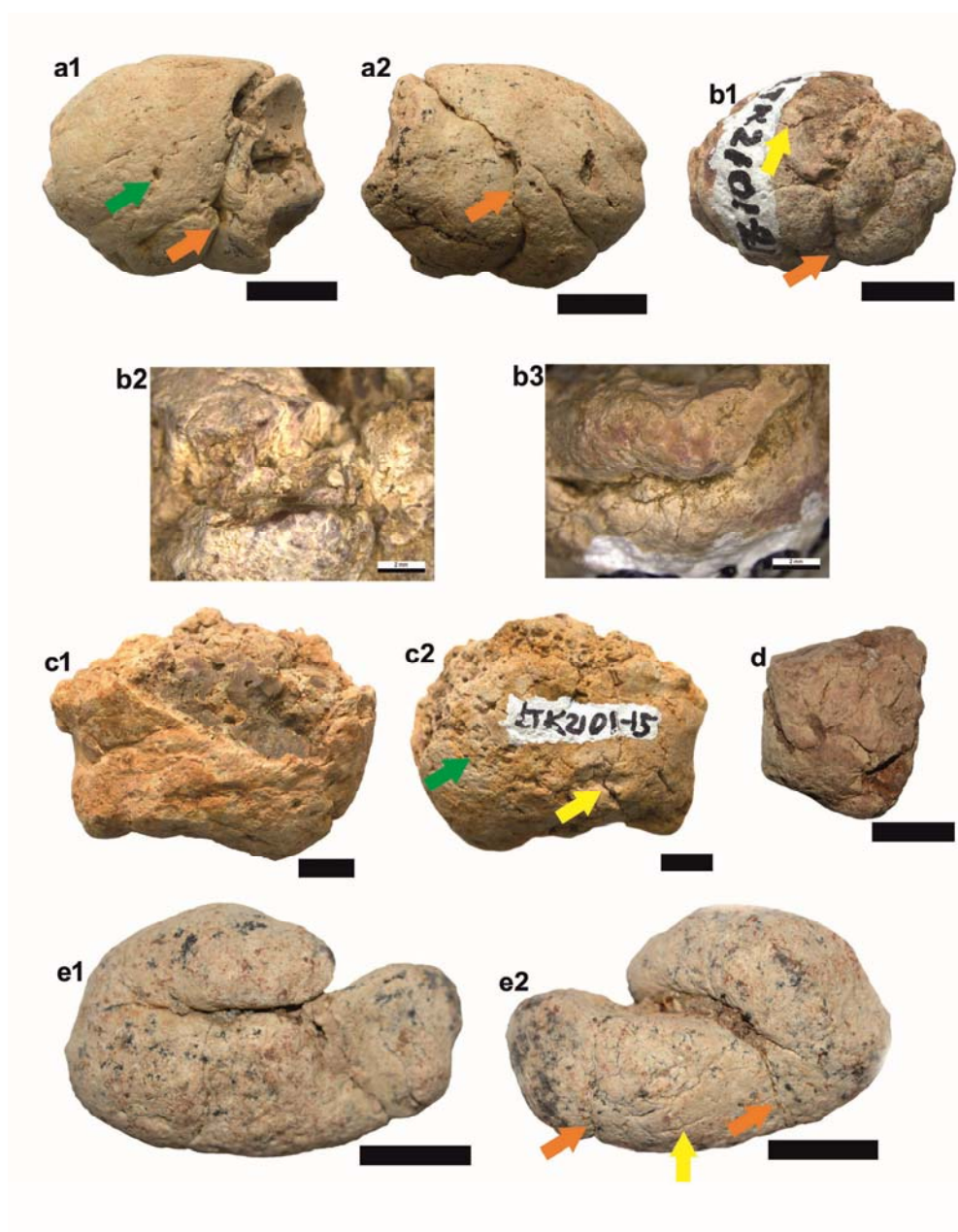


**Fig.3.** Digital photographs of late Cretaceous (Maastrichtian) coprolite specimens recovered from the intertrappean deposit at Lotkheri, central India. (a-b)Elliptical Morphotype M3,a1-a2. specimen no. LTK/2101-88 (BSIP 42262), b1-b3. specimen no. LTK/2101-21 (BSIP 42263). (c-d)Cylindrical Morphotype M4.[(c1-c2. specimen no. LTK/2101-15 (BSIP 42265);d. specimen no. VVK/BNP/GEO9 (BSIP 42264)]. (e) Irregularly folded Morphotype M5.[(e1-e2. specimen no. VVK/BNP/GEO10 (BSIP 42266)]. Note: b2-b3 are close-up views showing bone matter (reddish pink colour) embedded on the external surface of the coprolite specimen no. LTK/2101-21 (BSIP 42263). The green arrow marks burrow structures, the yellow arrow marks desiccation cracks, and the orange arrow marks constrictions. The scale bar equals 1 cm for all.





**Fig. 4.** Digital photographs of the late Cretaceous (Maastrichtian) vertebrate remains recovered from the intertrappean deposit at Lotkheri, central India. (a-b) *Chelonia* gen. et sp. indet. (a). carapace fragment, specimen no. LTK/2013-5 (BSIP 42267); (b). isolated vertebra, specimen no. LTK/2101-118 (BSIP 42268). (c-f) dermal scutes, *Crocodylia* gen. et sp. indet. (c). specimen no. LTK/2013-12 (BSIP 42269); d. specimen no. LTK/2013-18 (BSIP 42270); e. specimen no. LTK/2013-1 (BSIP 42271); f. specimen no. LTK/2013-19 (BSIP 42272). (g-m) isolated teeth, *Crocodylia* gen. et sp. indet. (g. specimen no. LTK/2013-13 (BSIP 42273); h. specimen no. LTK/2013-11 (BSIP 42274); i. specimen no. LTK/2013-10 (BSIP 42275); j. specimen no. LTK/2013-9 (BSIP 42276); k. specimen no. LTK/2013-16 (BSIP 42277); l. specimen no. LTK/2013-17 (BSIP 42278); m. specimen no. LTK/2013-15 (BSIP 42279)). (n-p) isolated scales, *Lepisosteus indicus* (n. specimen no. LTK/2101-266 (BSIP 42280); o. specimen no. LTK/2013-4 (BSIP 42281); p. specimen no. LTK/2013-2 (BSIP 42282)). The scale bar equals 1 cm for all.

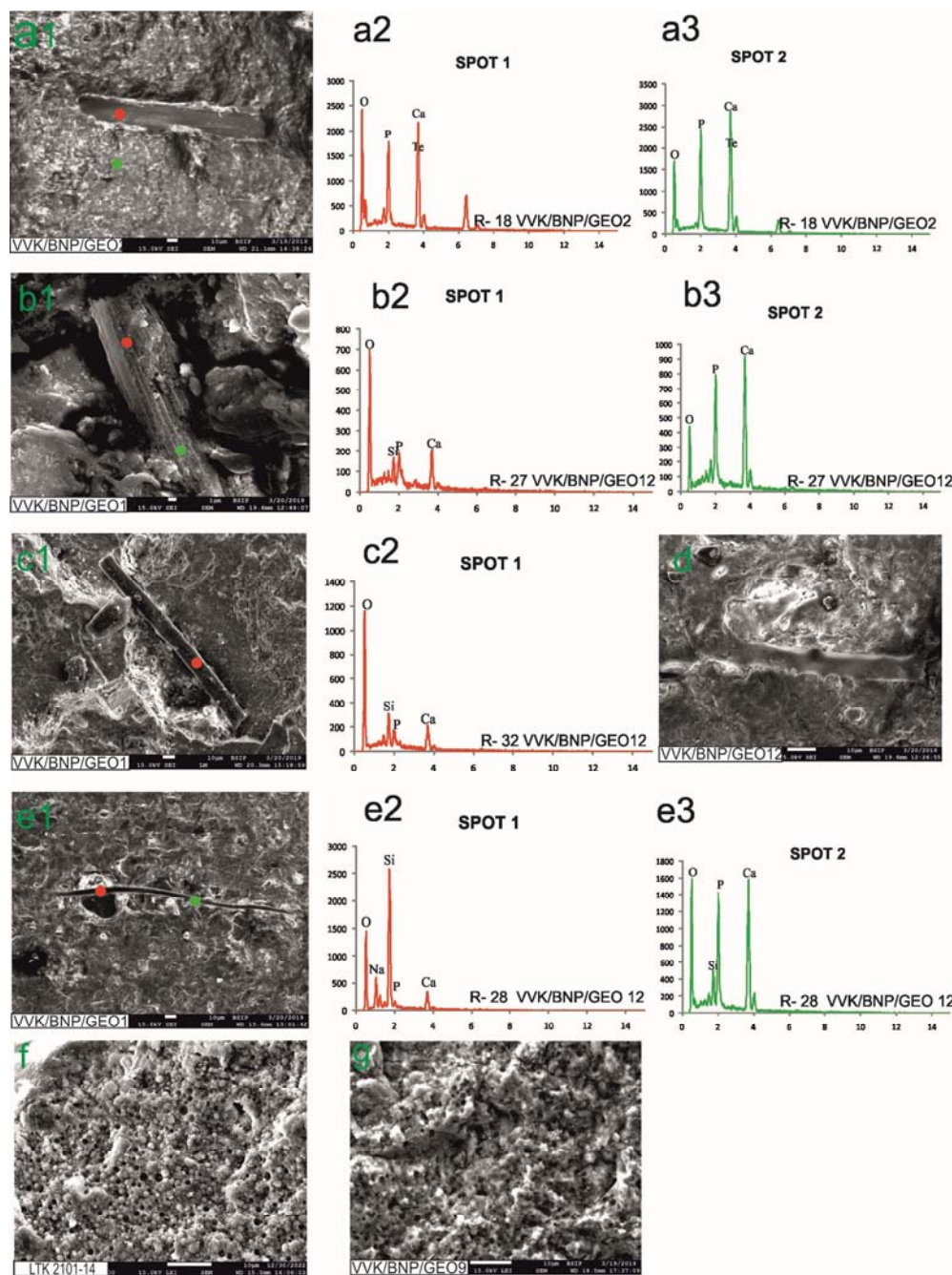


**Fig. 5:** Scanning electron microphotographs showing biotic inclusions and corresponding Energy Dispersive Spectroscopy (EDS) plots of the late Cretaceous (Maastrichtian) coprolites recovered from the intertrappean deposit at Lotkheri, central India. (a1-a3). Spherical Morphotype M1, specimen no. VVK/BNP/GEO2 (BSIP 42256), a1. bone fragment, a2. EDS data for spot 1, a3. EDS data for spot 2. (b1-b3) Spherical Morphotype M1, specimen no. VVK/BNP/GEO1 (BSIP 42253), b1. bone fragment, b2. EDS data for spot 1, b3. EDS data for spot 2. (c1-c2) Spherical Morphotype M1, specimen no. VVK/BNP/GEO1 (BSIP 42253), c1. bone fragment, c2. EDS data for spot 1. (d) Tear Drop shaped Morphotype M3, bone fragment, specimen no. VVK/BNP/GEO12 (BSIP 42257). (e1-e3) Spherical Morphotype M1, specimen no. VVK/BNP/GEO1 (BSIP 42253), e1. Sponge spicule fragment, e2. EDS data for Spot 1, e3. EDS data for Spot 2. (f) Microspherulites (egg-like mineral spheres), Tear Drop shape Morphotype M2, specimen no. LTK/2101-14 (BSIP 42259). g. Microspherulites (egg-like mineral spheres), Cylindrical Morphotype M4, specimen no. VVK/BNP/GEO9 (BSIP 42264). For details refer to Supplementary Data S1.



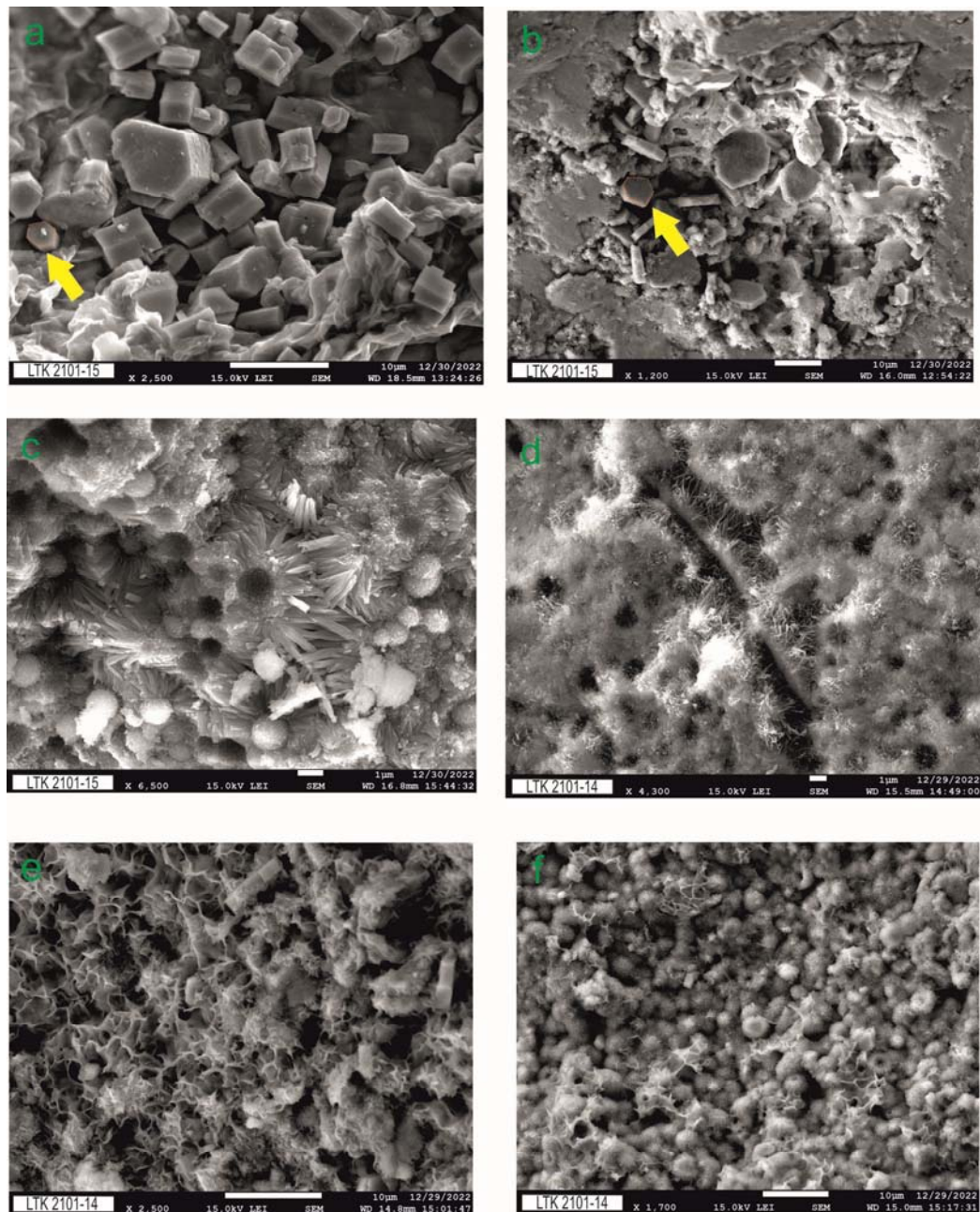


**Fig. 6.** Scanning electron microphotographs showing the internal texture and the Hydroxyapatite (HAP) crystals (as inclusions) within the late Cretaceous (Maastrichtian) coprolites recovered from the intertrappean deposit at Lotkheri, central India. (a-c) Cylindrical Morphotype M4, specimen no. LTK/2101-15 (BSIP 42265). (d-f) Tear Drop shaped Morphotype M3, specimen no. LTK/2101-14 (BSIP 42259). Note: Yellow arrow marks the hexagonal rod-shaped geometry of the HAP crystals. Needle-shaped geometry of the HAP crystals in c & d. Micron-sized spherical geometry of HAP crystals in e & f.

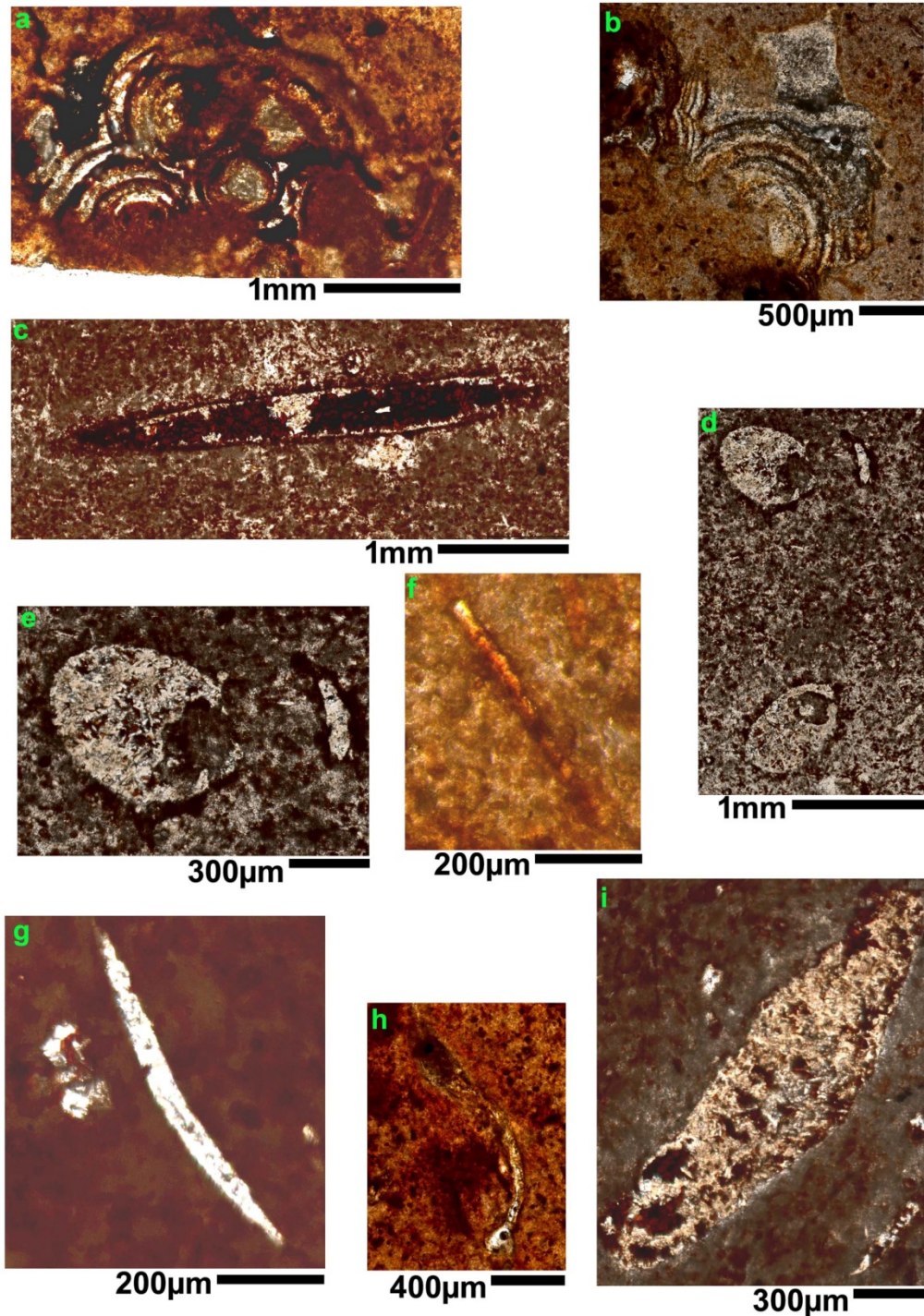


**Fig. 7.** Digital scans of the thin sections showing the biotic inclusions within the late Cretaceous (Maastrichtian) coprolites recovered from the intertrappean deposit at Lotkheri, central India. (a-b) Fish scales, Teardrop-shaped Morphotype M2, specimen no. LTK/2101-14 (BSIP 42259). (c) a cavity or a burrow structure, Cylindrical Morphotype M4, specimen no. LTK/2101-15 (BSIP 42265). (d-e) egg-like structures possibly of a dung beetle, Cylindrical Morphotype M4, specimen no. LTK/2101-15 (BSIP 42265). (f) bone fragment, Teardrop-shaped Morphotype M2, specimen no. LTK/2101-14 (BSIP 42259). (g) freshwater sponge spicule morphotype Acanthoxea, Cylindrical Morphotype M4, specimen no. LTK/2101-15 (BSIP 42265). (h) bone fragment, Teardrop-shaped Morphotype M2, specimen no. LTK/2101-14 (BSIP 42259). (i) burrow structure, Cylindrical Morphotype M4, specimen no. LTK/2101-15 (BSIP 42265).



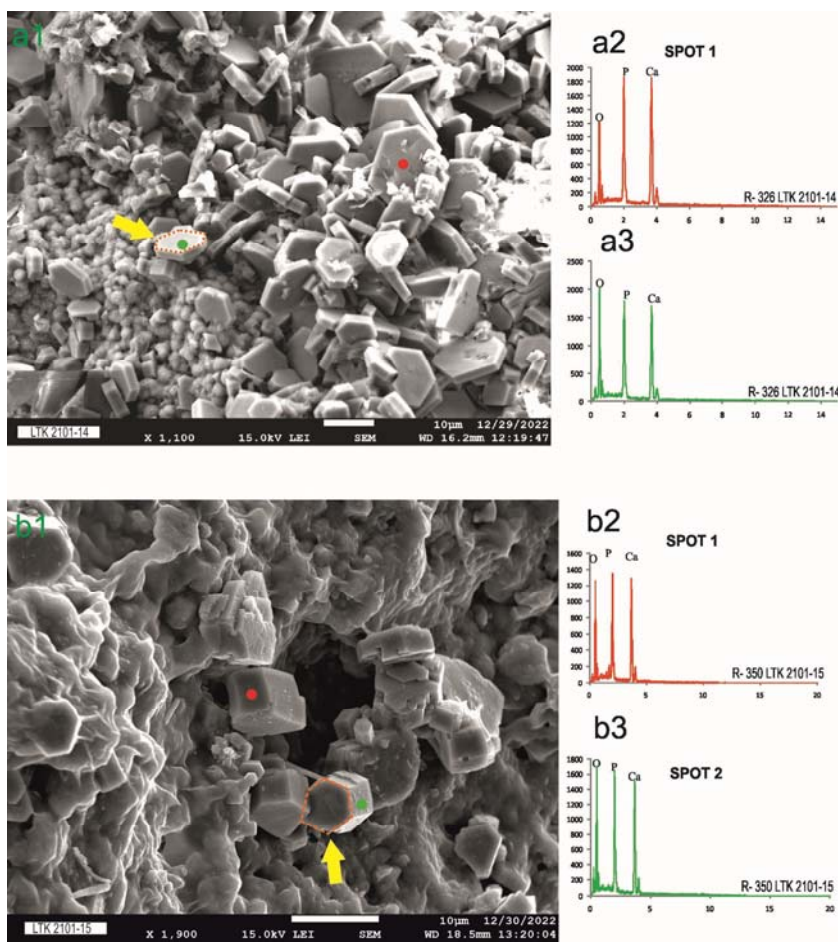


**Fig. 8.** Scanning electron microphotographs showing Hydroxyapatite (HAP) crystals and corresponding Energy Dispersive Spectroscopy (EDS) plots of the late Cretaceous (Maastrichtian) coprolites recovered from the intertrappean deposit at Lotkheri, central India. (a1-a3). Teardrop-shaped Morphotype M2, specimen no. LTK/2101-14 (BSIP 42259), a1. Rod-shaped HAP crystals, a2. EDS data for spot 1, a3. EDS data for spot 2. (b1-b3) Cylindrical Morphotype M4, specimen no. LTK/2101-15 (BSIP 42265), b1. Rod-shaped HAP crystals, b2. EDS data for spot 1, b3. EDS data for spot 2. Note: Yellow arrow marks the hexagonal rod-shaped geometry of HAP crystals.

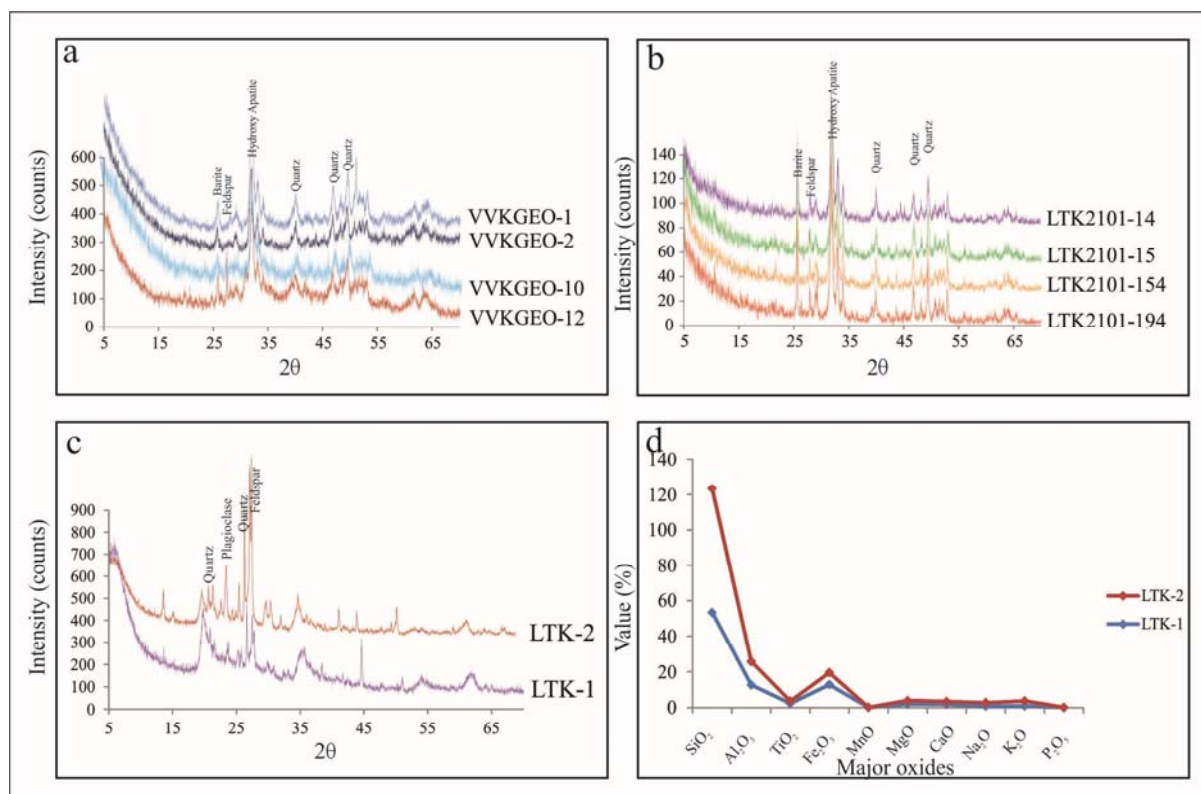


**Fig. 9.** Geochemical data of the late Cretaceous (Maastrichtian) coprolites, associated (LTK-1) and host (LTK-2) intertrappean sediments from Lotkheri, central India. (a-b) XRD spectra of coprolites. (c) XRD spectra of associated (LTK-1) and host (LTK-2) lithology. (d) XRF data on major oxides of associated (LTK-1) and host (LTK-2) lithology.

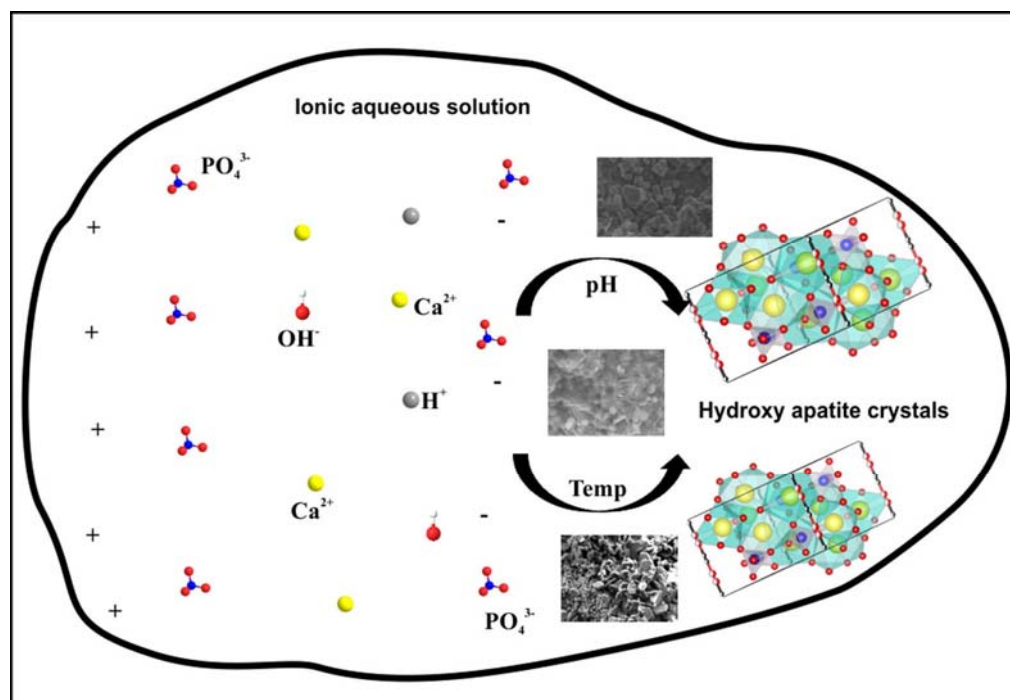


**Fig. 10.** Schematic diagram for the Growth Unit Model showing the presence of  $\text{Ca}^{2+}$ ,  $\text{PO}_4^{3-}$ , and  $\text{H}^+$ / $\text{OH}^-$  ions constituting the growth units that form the three different types i.e., spherical-, rod-, and needle-shaped geometry of Hydroxyapatite (HAP) crystals in coprolites.



## 780 EXPLANATION OF TABLE

S. No.	Morphotype(s)	Specimen	Length (in mm)	Width (in mm)	Length/Width	Avg Length (in mm)	Avg.Width (in mm)	Remarks
1	M1 (Spherical)	LTK/2101-154 (BSIP 42254)	30.16	24.18	1.25	26.46	23.17	Fig. 2a
2		LTK/2101-234 (BSIP 42255)	26.78	21.72	1.23			Fig.2b
3		VVK/BNP/GEO2 (BSIP 42256)	20.58	22.35	0.92			Fig. 2c
4		VVK/BNP/GEO1 (BSIP 42253)	28.33	24.44	1.16			Fig. 2d
5	M2 (Teardrop)	LTK/2101-194 (BSIP 42258)	33.44	24.66	1.36	37.97	32.38	Fig. 2e
6		LTK/2101-351 (BSIP 42260)	17.39	11.94	1.46			Fig. 2f1-f2
7		VVK/BNP/GEO12 (BSIP 42257)	33.12	54.37	0.61			Fig. 2g
8		LTK/2101-321 (BSIP 42261)	18.15	13.15	1.38			Fig. 2h1-h2
9		LTK/2101-14 (BSIP 42259)	87.77	57.78	1.52	-	-	Fig. 2i1-i2
10	M3 (Elliptical)	LTK/2101-88 (BSIP 42262)	31.68	23.14	1.37	29.71	22.58	Fig. 3a1-a2
11		LTK/2101-21 (BSIP 42263)	27.74	22.01	1.26			Fig. 3b1-b3
12	M4 (Cylindrical)	LTK/2101-15 (BSIP 42265)	59.78	42.39	1.41	40.42	30.93	Fig. 3c1-c2
13		VVK/BNP/GEO9 (BSIP 42264)	21.05	19.47	1.08			Fig. 3d
14	M5 (Irregular)	VVK/BNP/GEO10 (BSIP 42266)	36.66	13.33	2.75	-	-	Fig. 3e1-e2

**Table 1.** Measurements (length, width, length/width) data for the late Cretaceous (Maastrichtian) coprolites recovered from the intertrappean deposit at Lotkheri, central India.